Desalination and Water Treatment
www.deswater.com

doi: 10.1080/19443994.2015.1087342

57 (2016) 17944–17954
August

Taylor & Francis
Taylor & Francis Group

Improving the properties of an anion exchanger based on sugarcane bagasse by applying pretreatment methods

Yanpeng Mao[a], Miaomiao Zhang[a], Dingyi Yu[b], Wenlong Wang[a], Zhanlong Song[a], Xiqiang Zhao[a], Qinyan Yue[c,*]

[a]*National Engineering Laboratory For Coal-Fired Pollutants Emission Reduction, School of Energy and Power Engineering, Shandong University, Jinan 250100, P.R. China, Tel. +86 53188399372; Fax: +86 53188395877; emails: maoyanpeng@sdu.edu.cn (Y. Mao), zhangmiaomiaosdu@126.com (M. Zhang), wwenlong@sdu.edu.cn (W. Wang), zlsong@sdu.edu.cn (Z. Song), zxq@sdu.edu.cn (X. Zhao)*

[b]*School of Botany, The University of Melbourne, Victoria 3010, Australia, Tel. +61 451271106; email: dingyiyu08@gmail.com*

[c]*School of Environmental Science and Engineering, Shandong University, Jinan 250100, P.R. China, Tel. +86 53188365258; Fax: +86 53188365258; email: qyyue58@aliyun.com*

Received 6 March 2015; Accepted 21 August 2015

ABSTRACT

Sugarcane bagasse (SB) was pretreated using the microwave-induced hydrothermal method (MIHM), ultrasonic pretreatment, dilute-acid hydrolysis, and organosolv processes, and subsequently modified using a combination of epichlorohydrin, N,N-dimethylformamide, ethylenediamine, and triethylamine to synthesize anion exchangers. The characteristics of AE with different pretreatment methods were investigated using proximate and ultimate analysis, Zeta potential, and Fourier transform infrared spectroscopy. The kinetics of nitrate removal by different AE at a pH of 7.0 were well linearized with a pseudo-second-order kinetic model and thermodynamics at pH of 4.0 and 7.0 was best fitted using Langmuir isotherm and the Dubinin–Radushkevich model. Results confirmed that all pretreatments enhanced the modification of SB and that the optimum pretreatment was MIHM, with the highest nitrogen content (8.20%) and nitrate sorption capacity (95.7 mg/g at pH 4.0 and 100.2 mg/g at pH 7.0).

Keywords: Sugarcane bagasse; Pretreatment; Anion exchangers; Nitrate removal

1. Introduction

Sugarcane bagasse (SB), one of the largest agriculture wastes obtained from the cane pulp after sugar extraction [1,2], has a dominant composition of cellulose, hemicelluloses, and lignin [3,4], and hence, the potential to be used or modified as an effective adsorbent to remove pollutants from contaminated water, with the added benefits of being inexpensive and recyclable [5]. Studies have investigated the thiol-functionalized SB for the adsorption of mercury [6] and arsenic [7], the amine-functionalized SB for the adsorption of anion ions [8–11], and other chelate-functionalized SB for the adsorption of mercury [12].

The amine-functionalized modification of agricultural residues (AR) was initially established as the EDM method by Orlando et al. [8,9], which cross-linked AR with epichlorohydrin and dimethylamine

*Corresponding author.

in the presence of N,N-dimethylformamide using pyridine as a catalyst. Subsequently, a modified method, i.e. the ETM method, which altered AR with epichlorohydrin, ethylenediamine, triethylamine, and N,N-dimethylformamide, was developed by Wang et al. [11]. The ETM method has been widely used to modify wheat residue [13], pine sawdust and bark, spruce bark, birch bark, peat [14], and pine sawdust [15]. Recently, the developments of amine-functionalized lignocellulosic materials took two distinct directions. First, additional chemicals were added based on the ETM method. A new amine-functionalized corn stalk with magnetic property was developed by adding iron oxide (Fe_3O_4) nanoparticles [16]. Second, chemicals in the ETM method were replaced by less hazardous chemicals. Normally, N-(3-chloro-2-hydroxypropyl) trimethyl ammonium chloride was used as a substitute to modify lignocellulosic materials [17,18].

Cellulose, hemicelluloses, and lignin in AR contain a significant amount of hydroxyl groups that can be used to prepare certain functional polymers [19,20]. However, the chemicals used in amine-functionalized modification of AR were inefficient, as the complex and crystalline structure of AR, which makes the fiber in AR dense and impermeable [21], would reduce the accessibility of hydroxyl groups to chemicals, and consequently, affect the yield and the reactivity of the amine-functionalized AR. In addition, to obtain successful adsorption capacity of product, large amounts of chemicals would be required, which would produce more waste residuals. Significantly, the adsorption capacity of the product remained almost constant when the addition of chemicals further increased [19]. To decrease crystalline cellulose and improve the porosity of a material, several pretreatments classified as chemical, physical, and physicochemical methods have been investigated for bioethanol processing [22–24]. However, little research has been performed on the pretreatments of AR used in the amine-functionalized modification to increase the effective reactions between chemicals and AR, which will be investigated in this study.

In the present study, several pretreatments, including the microwave-induced hydrothermal method (MIHM) [21,25], ultrasonic pretreatment (UP) [26], dilute-acid hydrolysis (DH) [23], and organosolv processes (OP) [24], have been performed and modified to avoid a significant loss of SB due to hydrolysis. Following the process of pretreatments, various materials were modified to anion exchangers (AE) by using the ETM method. The characteristics and nitrate adsorption ability of AE were studied to provide new insight into the chemical modification of SB. The pretreatments could be beneficial in improving the chemical modification of SB, and hence decrease the loss of chemicals and improve the nitrate adsorption ability of AE.

2. Materials and methods

2.1. Materials

Analytical grade reagents were used in all experiments and were purchased from Tianjin Kemiou Chemical Reagent Company Limited unless otherwise stated. All solutions were prepared using 18 MΩ cm ultrapure Milli-Q (MQ) water. The raw SB, obtained from Huaan, Guangxi, China, was washed with MQ water, dried at 60˚C for 12 h, and sieved into particles less than 250 μm in diameter.

2.2. Pretreatment of SB

To destroy the crystalline structure and improve the porosity of SB, the SB was pretreated by two physical methods and two chemical methods, as follows: using the MIHM, 5 g of SB were added into 100 mL MQ water and the mixture was heated for 15 min using the irradiation of a 2,450 MHz microwave with 900 W of power; using UP, 5 g of SB were washed for 20 min with 100 mL MQ water in an 20 kHz ultrasonic radiator; using DH, 5 g of SB reacted with 100 mL 1.2% v/v H_2SO_4 solution for 20 min at 100˚C; using the OP, 5 g of SB were mixed with 100 mL of 20% v/v acetone solution for 20 min at 80˚C. Following pretreatment, the pretreated SB (PSB), filtered through 0.45 μm pore size membrane filters, was washed twice with ethyl alcohol (50% w/w) and MQ water, and then dried at 60˚C in a vacuum drier for 12 h.

2.3. Preparation of AE using SB and PSB

Preparation of AE using SB and PSB were based on the ETM method [13]. One gram of SB or PSB was added to 10 mL of epichlorohydrine and 12 mL of N, N-dimethylformamide in a 250 mL three-neck round bottom flask. The mixture was stirred for 60 min and the temperature was maintained at 90˚C, which was proved to be the optimal temperature in our study (results not shown). An aliquot of 2 mL of ethylenediamine was added and the solution was stirred for 60 min, followed by the addition of 10 mL of 99% triethylamine (w/w) and a stirring of the mixture for 120 min. The product was washed with 500 mL of ethyl alcohol (50% w/w) and MQ water to remove the residual chemicals, dried at 60˚C for 12 h, and sieved to obtain particles smaller than 250 μm in diameter.

2.4. Loss of SB and yield of AE

The loss of SB (L, %) in the process of pretreatment and the yield of AE (Y, %) from SB were determined gravimetrically using the following equations:

$$L(\%) = (m_0 - m_1)/m_0 \times 100 \quad (1)$$

$$Y(\%) = m_2/m_1 \times 100 \quad (2)$$

where m_0, m_1, and m_2 are the dry weights of SB, PSB, and AE, respectively.

2.5. Characterization of SB and AE

2.5.1. Proximate and ultimate analysis

The proximate composition, i.e. fixed carbon, fugitive constituent, ash, and moisture, and the ultimate composition, i.e. carbon (C), hydrogen (H), and nitrogen (N), were determined for dry SB, PSB, and AE, and changes in composition during the processes of pretreatment and preparation were recorded. The proximate analysis and ultimate analysis were performed using a SDTGA5000 (Hunan Sande Co., Ltd, China) and a vario EL cube (Elementar, Germany), respectively.

2.5.2. Zeta potential

The specimens of SB, PSB, and AE were dispersed in the MQ water to make the particles visible under the microscope, and Zeta potential measurements were performed at a pH of 7.0 using a JS94H microelectrophoresis apparatus (Shanghai Zhongchen Digital Technical Apparatus Co., Ltd, China).

2.5.3. FTIR spectra

The chemical structure and functional groups in SB, PSB, and AE were determined using a Nicolet 6700 FTIR (Thermo Fisher Scientific, United States). The wave number range was from 4,000 to 400 cm^{-1}, and the optical grade potassium bromide (KBr), dried at 80℃ for 8 h before used, was selected as a spectroscopically matrix.

2.6. Nitrate removal by AE

2.6.1. Effect of different parameters on nitrate removal

In this study, AE dosage, initial pH, and contact time were selected as experimental parameters.

A small amount (0–5.0 g/L) of AE was added to 100 mL 50 mg/L nitrate (noted as NO_3^-) solution with varying pH (2.0–10.0) in Pyrex® vessels (250 mL conical flask). The pH value was measured using a PHS-3C pH meter (Shanghai, China) combined with a glass electrode and Ag/AgCl reference. It should be noted that the pH was adjusted to the desired value without the addition of a buffer, and hence, the pH of the dye solutions was evaluated again to confirm that there was minimal change (~ ±1.4) in the pH after completion of the static adsorption experiment (Fig. 1). In this study, the initial pH values were taken as the "true" values of the investigated solutions. The removal of nitrate from the solution using PSB-AE was performed using a horizontally rotating shaker for 60 min at 25℃. It is noteworthy that the nitrate adsorption by AE has been proved to increase with an increase in temperature [27]. Therefore, only room temperature (T = 25℃) was used to evaluate the nitrate removal ability of AE in this study. Samples were pipetted (using a 3 mL syringe) at appropriate time intervals and immediately separated by filtration through a 25 mm diameter 0.45 μm membrane filter, and the residual nitrate was analyzed colormetrically using UV–vis spectrophotometry (TU-1901, Persee, China).

The nitrate removal efficiency (R, %) was determined as a percentage with the following equation:

$$R = \frac{C_0 - C_r}{C_0} \times 100 \quad (3)$$

where C_0 (mg/L) is the initial nitrate concentration and C_r (mg/L) is the residual nitrate concentration.

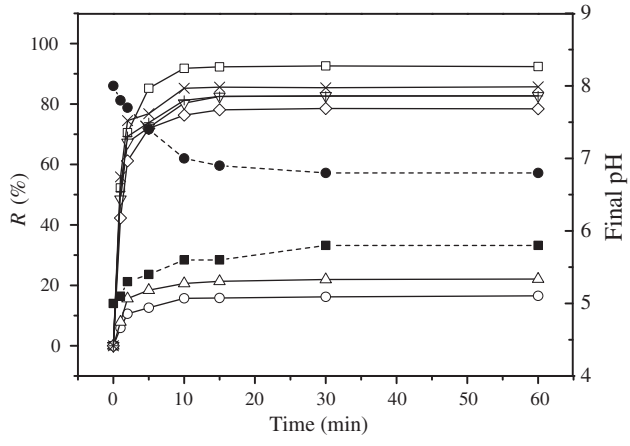

Fig. 1. Left Y axis (solid lines): Effect of contact time on the removal of nitrate by SB (○), PSB_{MIHM} (△), SB-AE (◇), PSB_{DH}-AE (▽), PSB_{OP}-AE (+), PSB_{UP} -AE (×), and PSB_{MIHM}-AE (□) at initial pH 7.0. Right Y axis (dashed lines): Effect of contact time on pH changes with initial pH 5.0 (■) and 8.0 (●). Initial nitrate concentration 50 mg/L, stirring rate 120 r/min, resin dose 4 g/L, and T = 25℃.

2.6.2. Nitrate sorption capacity of AE

A certain amount of AE (0.4 g) was mixed with 100 mL nitrate concentrated solutions (10–100 mg/L) and the mixture was shaken at initial pH 7.0 and $T = 25$℃ in a stirrer operating 120 rpm for 12 h to ensure equilibrium. The nitrate sorption capacity q (mg/g) of AE was calculated as follows:

$$q = \frac{(C_0 - C_r) \times V}{m} \tag{4}$$

where V (L) is the volume of the mixture and m (g) is the mass of the PSB-AE in the batch mixture.

2.6.3. Kinetics models

When treating nitrate sorption as a second-order process, the relationship of sorption capacity (q_t, mg/g) and adsorption time (t, min) can be linearly expressed as follows [28]:

$$\frac{t}{q_t} = \frac{1}{k_2 q_e^2} + \frac{t}{q_e} \tag{5}$$

where k_2 (g/mg/min) represents the second-order rate constant and q_e (mg/g) is the sorption capacity at adsorption equilibrium. The initial adsorption rate h (g/mg/min) can be calculated using the following equation [28]:

$$h = k_2 q_e^2 \tag{6}$$

Recognizing that the kinetics of nitrate sorption may be controlled by diffusion processes, the intra-particle diffusion model introduced by McKay and Poots [29] was expressed as follows:

$$q_t = k_i t^{1/2} + C \tag{7}$$

where C (mg/g) is the intercept and k_i (mg/g/min) is the intra-particle diffusion rate constant.

2.6.4. Adsorption isotherms

The adsorption isotherm of nitrate onto PSB-AE at 25℃ was evaluated using three sorption isotherm models, including Langmuir isotherm, Freundlich isotherm, and Dubinin–Radushkevich (D–R) model [28,30,31], which are represented mathematically in Table 1.

3. Results and discussion

3.1. Loss of SB and yield of AE

Pretreatment of SB disrupted the crystalline structure of biomass to make cellulose and lignin more accessible, and inevitably transferred substance from solid to liquid to result in a loss of SB. As shown in Table 2, the pretreatment of UP and OP result in the least and the greatest loss of SB with 2.1 and 18.1%, respectively. It should be noted that the loss of SB is overestimated in this study because a small amount of SB was lost in the process of filtration. It was evident in both cases that pretreatment markedly increased the yield of AE by a minimum improvement of 49.5% using DH and the maximum improvement of 121.9% using MIHM. The results showed that the pretreatment was beneficial to the production of AE by exposing more hydroxyl groups to chemicals, and further indicated that the best pretreatment for SB was MIHM, which brought the maximum improvement of the yield of AE but did not result in significant loss of SB.

Table 1
Mathematical expression for sorption isotherm models

Sorption isotherms	Non-linear expression	Linear expression
Langmuir isotherm	$q_e = \frac{K_L q_m C_e}{1+K_L C_e}$	$\frac{C_e}{q_e} = \frac{C_e}{q_m} + \frac{1}{q_m K_L}$
Freundlich isotherm	$q_e = K_F C_e^{1/n}$	$\ln q_e = \ln K_F + \frac{1}{n} \ln C_e$
D–R model	$\frac{q_e}{q_{m(D-R)}} = \exp(-\beta\varepsilon^2)$	$\ln q_{e(D-R)} = \ln q_{m(D-R)} - \beta\varepsilon^2, \quad E = \frac{1}{\sqrt{2\beta}}$

Notes: q_e (mg/g): the sorption capacity at adsorption equilibrium, C_e (mg/L): the sorbate equilibrium concentration in liquid phases, q_m (mg/g): the capacity of the sorbent, K_L (L/mg): the constant of the Langmuir isotherm, K_F (mg/g) (l/mg)$^{1/n}$: the constant of the Freundlich isotherm, n: Heterogeneity factor, $q_{m(D-R)}$ (g/g): the theoretical saturation capacity in D–R equation, β (mol^2/kJ^2): the constant related to the sorption energy, ε: the Polanyi potential is equal to $-RT \ln (1 + 1/C_e)$, E (kJ/mol): the mean of free adsorption energy.

Table 2
The characterization and the nitrate removal ability of different materials

Process	Materials		Loss and yield (%)		Proximate analysis (wt.%)				Ultimate analysis (wt.%)			Zeta potential (mV)	*R* (%)
			L	*Y*	FC	F	A	M	C	H	N		
	SB		–	–	16.2	71.1	6.6	6.1	40.7	5.6	0.94	−30.2	16.5
Pretreatment	PSB	PSB_{MIHM}	6.2	–	20.6	67.5	5.2	6.7	42.1	5.9	0.61	−30.9	22.1
		PSB_{UP}	2.1	–	17.8	69.3	6.9	6.0	40.8	5.1	0.88	−31.8	–
		PSB_{DH}	12.8	–	17.9	71.5	4.1	6.5	43.8	6.2	0.64	−33.0	–
		PSB_{OP}	18.1	–	24.3	62.1	7.1	6.5	43.5	5.9	0.72	−30.9	–
Modification	AE	SB-AE	–	347.0	12.4	72.5	7.1	8.0	43.2	6.8	6.45	+5.4	78.4
		PSB_{MIHM}-AE	–	468.9	8.2	78.1	6.0	7.7	46.5	6.4	8.20	+6.9	92.4
		PSB_{UP}-AE	–	418.7	9.5	74.9	6.4	9.2	45.3	6.0	8.09	+6.9	85.7
		PSB_{DH}-AE	–	396.5	11.8	73.4	6.4	8.4	44.1	6.5	7.22	+6.2	82.7
		PSB_{OP}-AE	–	400.8	14.1	71.1	6.7	8.1	45.0	6.6	7.01	+5.8	82.7

Notes: SB: sugarcane bagasse, PSB: pretreated SB, MIHM: microwave-induced hydrothermal method, UP: ultrasonic pretreatment, DH: Dilute-acid hydrolysis, OP: Organosolv processes, AE: anion exchanger, *L*: loss of SB, *Y*: yield of SB-AE, FC: fixed carbon, F: fugitive constituent, A: ash, M: moisture, *R:* removal efficiency of nitrate by absorbents in 60 min.

3.2. Characterization of SB and AE

The approximate and ultimate analyses of the different materials as well as Zeta potentials are presented in Table 2. In general, fixed carbon in PSB materials slightly increased by 1.6–8.1% after pretreatment of the SB raw material, and fixed carbon in the AE materials dramatically decreased by 2.8–12.4% with an increase of fugitive constituent (by 1.4–10%) after the modification of SB and PSB materials, as was expected. It is noteworthy that in the modification process, the range of changes of fixed carbon and the fugitive constituent in PSB-AE were higher than those in SB-AE, indicating that a modification can be heightened through pretreatment and MIHM offers the greatest promotion. In the ultimate analysis, a slight increase in the carbon content was observed in both pretreatment and modification. The nitrogen content of AE, however, increased significantly in the process of modification from 0.61–0.94% to 6.45–8.20% on average, indicating that amine groups had anchored onto the SB and PSB materials. The pretreatment of MIHM also resulted in the highest nitrogen content, which confirms that the reactions in modification proceeded more efficiently.

The Zeta potential of SB material at a pH of 7.0 slightly decreased from −30.2 to −30.9 to −33 mV after pretreatment. Through the process of modification, positive-charge functional groups in the framework of AE, i.e. amine groups, resulted in a significant increase in the Zeta potential of AE +5.4 to +6.9 mV.

The FTIR spectra of SB and PSB using MIHM, UP, DH, and OP are represented as lines A–E in Fig. 2, and the FTIR spectra of SB-AE and PSB_{MIHM}-AE

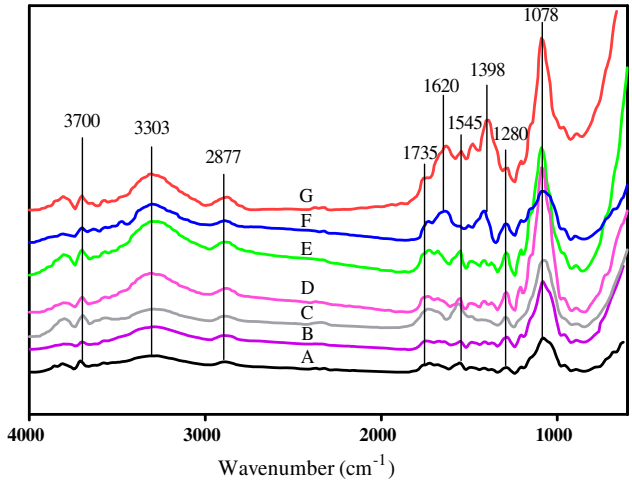

Fig. 2. FTIR spectra of SB (A), PSB_{MIHM} (B), PSB_{UP} (C), PSB_{DH} (D), PSB_{OP} (E), SB-AE (F), and PSB_{MIHM}-AE (G).

which exhibited the best nitrate removal efficiency, are represented as lines F and G in Fig. 2. The spectra of PSB did not show the formation of any new peaks after pretreatment, while the spectra of both SB-AE and PSB_{MIHM}-AE exhibited a sharp adsorption band at 1,398 cm^{-1}, indicating the presence of amine groups in PSB_{MIHM}-AE. Similar results were reported by Xu et al. [13], with grafted amine groups in WR-AE observed at the band of 1,371 cm^{-1}. The low and sharp band at 3,700 cm^{-1} was associated with the asymmetrical stretching of the O–H group [32], and the high and broad band at 3,303 cm^{-1} indicates the presence of the O–H stretching of the hydroxyl group and hydrogen bonds, which were related to a peak at

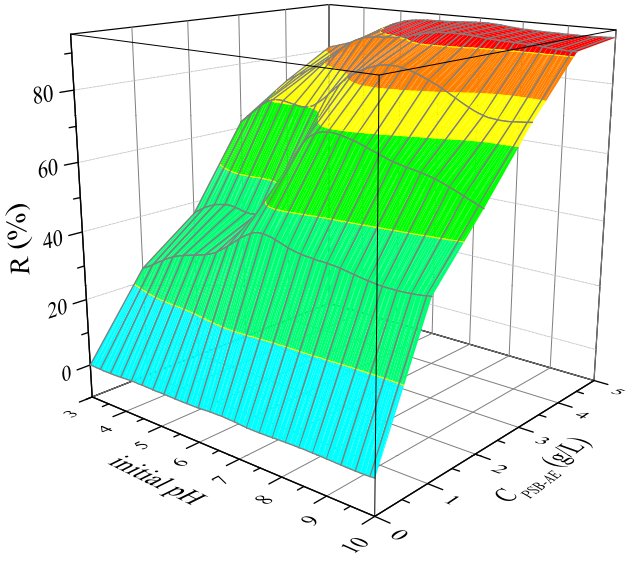

Fig. 3. Effects of initial pH and PSB-AE dosage on the removal of nitrate by PSB_{MIHM}-AE material. Initial nitrate concentration 50 mg/L, stirring rate 120 r/min, contact time 60 min, and T = 25°C.

3,200–3,600 cm^{-1} [33,34]. The absorption peaks around 2,877 cm^{-1} indicate the presence of a C–H stretching vibration [35], which is the skeleton structure of cellulose and hemicelluloses. The band at 1,735 cm^{-1} indicates the presence of acetyl groups of hemicelluloses [6]. The absorption peaks around 1,620 cm^{-1} for PSB_{MIHM}-AE and 1,545 cm^{-1} for SB-AE indicate the presence of aromatic skeletal vibration [32]. The maximum peak at 1,078 cm^{-1} was associated with the C–O stretching vibration in cellulose, hemicelluloses, and lignin [35]. The enhancement in the number of apparent peaks in the range of 600–1,700 cm^{-1} for PSB may be due to pretreatment causing the recovery in the number of chemical groups appearing in this specific range.

3.3. Nitrate sorption by AE

3.3.1. The effect of contact time

As shown in Fig. 1, nitrate removal efficiency increased dramatically by increasing the contact time within the first ten minutes. The reduction of nitrate by AE materials was rapid and the equilibrium was reached in the contact time of 30 min for all AE materials. In the rest of the experiments, 60 min was chosen for nitrate removal to ensure equilibrium.

3.3.2. The effect of pretreatments

As illustrated in Fig. 1, that nitrate removal efficiencies by 4 g/L AE materials in 60 min at a pH of 7.0 were dramatically higher than raw AE material (by 56.3–70.3%) and nitrate removal efficiencies by PSB-AE materials were also significantly higher than SB-AE materials (by 4.3–14.0%). It should be noted that material with a higher nitrate removal efficiency also has a higher nitrogen content (Table 2), indicating that the content of amine groups in materials introduced by modification, could be the functional groups in AE for nitrate reduction. The maximum enhancement of nitrate removal efficiency was the result of MIHM pretreatment, which was in accordance with the highest nitrogen content in the material of PSB_{MIHM}-AE. Hence, the experiments to select advisable parameters were conducted using PSB_{MIHM}-AE material.

3.3.3. The effect of pH and PSB-AE dosage

In the range of initial pH from 3.0 to 10.0, the enhancement of nitrate removal efficiency by 0 to 5 g/L PSB_{MIHM}-AE material in 60 min is shown in Fig. 3. At lower pH (<5.0), the nitrate removal efficiency decreased dramatically with the decrease of pH, which may be due to the competition of the functional groups

Table 3
Kinetics models for the removal of nitrate by different materials at initial pH 7.0

	Second-order kinetics				The intra-particle diffusion model		
Materials	q_e (mg/g)	k_2	h (g/mg/min)	R^2	k_i (mg/g/min)	C	R^2
SB	2.12	0.351	1.57	0.999	0.162	1.09	0.544
PSB_{MIHM}	2.83	0.301	2.41	0.999	0.201	1.57	0.479
SB-AE	9.91	0.198	19.5	0.999	0.504	6.90	0.412
PSB_{MIHM}-AE	11.7	0.188	25.6	0.999	0.581	8.24	0.415
PSB_{UP}-AE	10.8	0.256	29.8	0.999	0.407	8.36	0.401
PSB_{DH}-AE	10.5	0.183	20.0	0.999	0.493	7.47	0.466
PSB_{OP}-AE	10.4	0.220	23.9	0.999	0.443	7.77	0.433

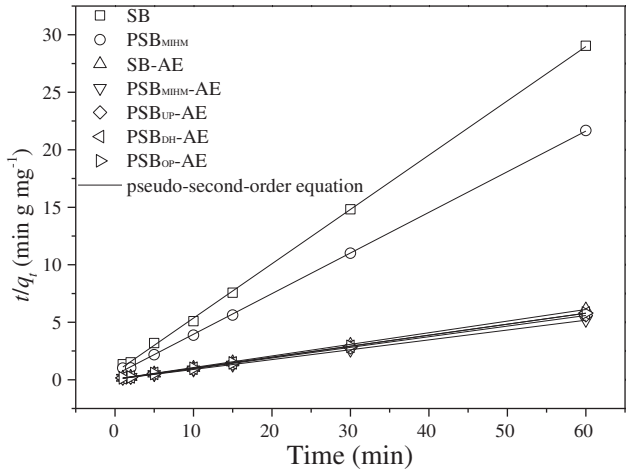

Fig. 4. Pseudo-second-order kinetics for the removal of nitrate by SB, PSB_{MIHM}, SB-AE, PSB_{DH}-AE, PSB_{OP}-AE, PSB_{UP}-AE, and PSB_{MIHM}-AE at initial pH 7.0. Initial nitrate concentration 50 mg/L, stirring rate 120 r/min, resin dose 4 g/L, and T = 25°C.

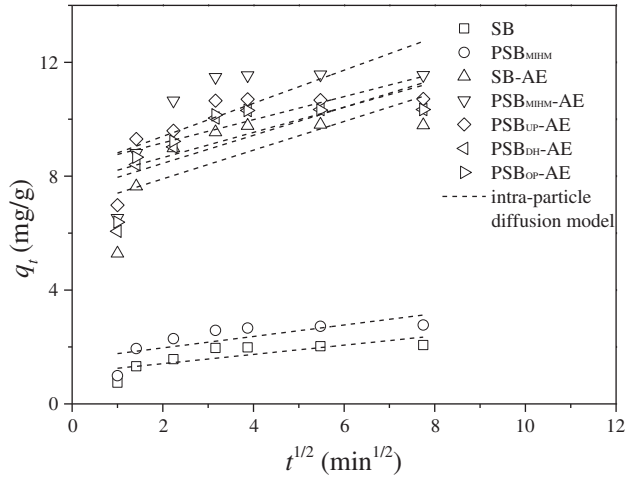

Fig. 5. Intra-particle diffusion model for the removal of nitrate by SB, PSB_{MIHM}, SB-AE, PSB_{DH}-AE, PSB_{OP}-AE, PSB_{UP}-AE, and PSB_{MIHM}-AE at initial pH 7.0. Initial nitrate concentration 50 mg/L, stirring rate 120 r/min, resin dose 4 g/L, and T = 25°C.

on the surface of PSB_{MIHM}-AE by the protonation reactions. At a higher pH (>5.0), the nitrate removal efficiencies of 88.1–93.1% were obtained, which means the nitrate reduction by PSB_{MIHM}-AE could be operated at a broad pH range, from 5.0 to 10.0.

3.4. Kinetics models of nitrate sorption by PSB-AE

Experiments were carried out to examine the rates of nitrate removal by different materials at an initial

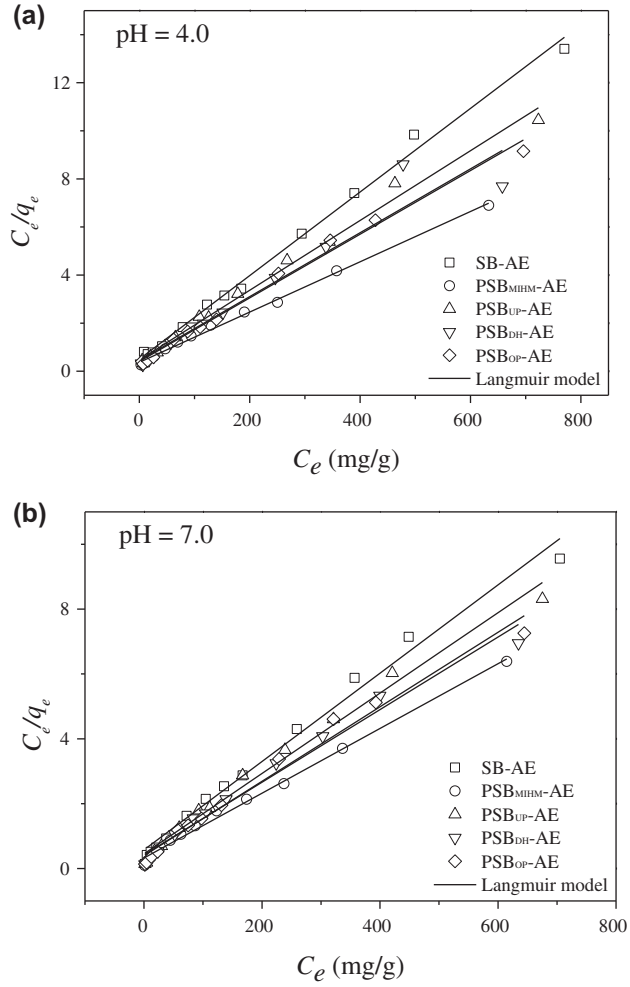

Fig. 6. Langmuir isotherm for the removal of nitrate by SB, PSB_{MIHM}, SB-AE, PSB_{DH}-AE, PSB_{OP}-AE, PSB_{UP}-AE, and PSB_{MIHM}-AE at initial pH 4.0 (a) and pH 7.0 (b). Initial nitrate concentration 50 mg/L, stirring rate 120 r/min, resin dose 4 g/L, and T = 25°C.

pH of 7.0. Table 4 demonstrates the extremely good linear relationship between time (t) and t/q_t with coefficients over 0.999 in our study. Second-order rate constants k_2 and sorption capacity q_e at adsorption equilibrium were determined directly from these plots and the calculated values are shown in Table 3. From this table, the effect of modification and pretreatment on nitrate adsorption is quantified using q_e, which dramatically increases after modification and slight increases after applying different pretreatments. Following modification, the k_2 value is observed to decrease dramatically while the h value increases dramatically. The effect of pretreatments on the values of k_2 is not significant, while the h value increases dramatically after applying different pretreatments. As such, the results suggest that the initial adsorption rate

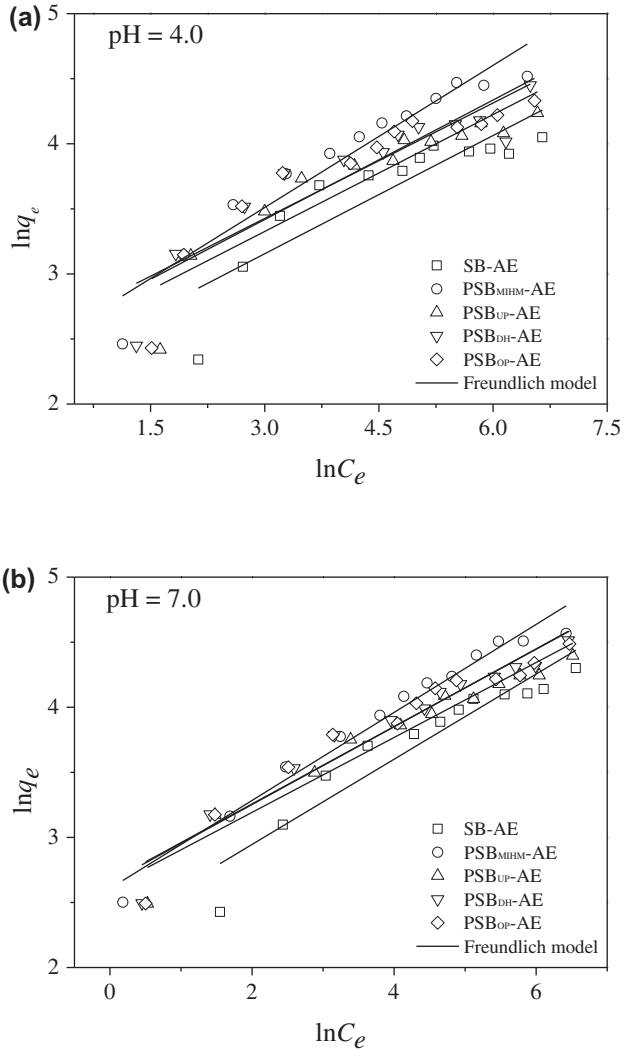

Fig. 7. Freundlich isotherm for the removal of nitrate by SB, PSB_{MIHM}, SB-AE, PSB_{DH}-AE, PSB_{OP}-AE, PSB_{UP}-AE, and PSB_{MIHM}-AE at initial pH 4.0 (a) and pH 7.0 (b). Initial nitrate concentration 50 mg/L, stirring rate 120 r/min, resin dose 4 g/L, and T = 25°C.

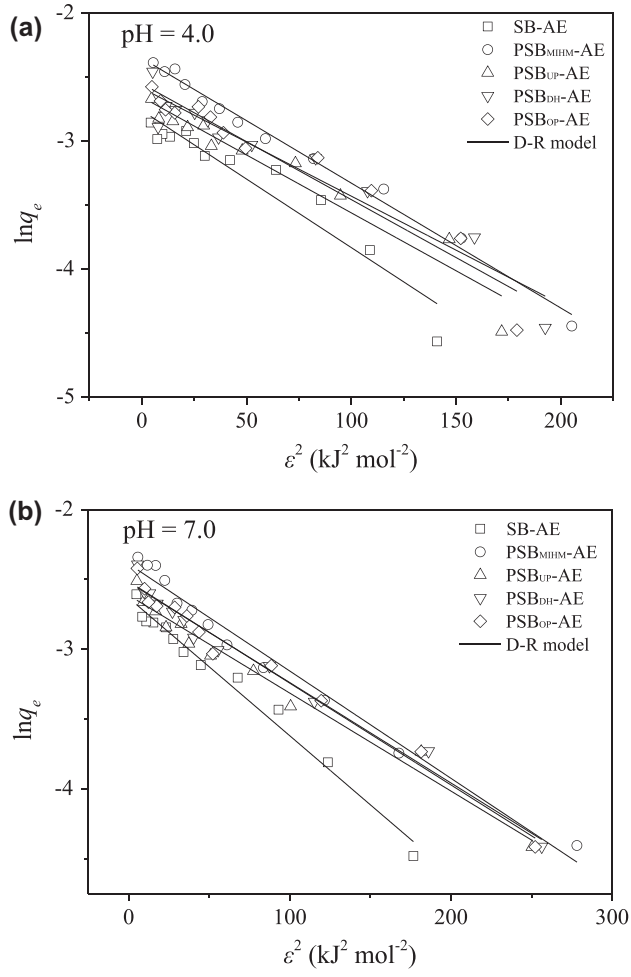

Fig. 8. D–R model for the removal of nitrate by SB, PSB_{MIHM}, SB-AE, PSB_{DH}-AE, PSB_{OP}-AE, PSB_{UP}-AE, and PSB_{MIHM}-AE at initial pH 4.0 (a) and pH 7.0 (b). Initial nitrate concentration 50 mg/L, stirring rate 120 r/min, resin dose 4 g/L, and T = 25°C.

was primarily determined by fast chemical reactions between nitrate and surface sites, which increase dramatically through modification and pretreatments, while subsequent the rates were most likely determined by physical diffusion effects (Fig. 4).

The intra-particle diffusion model was applied to assess the importance of intra-particle diffusion to the kinetics of nitrate removal by different materials. Values of the intra-particle diffusion rate constant, k_i, obtained by plotting q_t vs. $t_{1/2}$, are shown in Table 3. The linearized plots of the intra-particle diffusion model are presented in Fig. 5. As shown in Fig. 5, none of the plots passed through the origin, indicating that intra-particle diffusion was not the rate-limiting step for nitrate removal by different materials [36,37].

3.5. Adsorption isotherms of nitrate sorption by PSB-AE

The Langmuir isotherm, Freundlich isotherm, and the D–R model were used to describe adsorption isotherms of nitrate sorption by different materials at pH of 4.0 and 7.0 with reasonable linear relationships for the various sets of nitrate removal data (Figs. 6–8). The coefficients for different isotherms calculated from the intercepts and slopes of these straight lines are outlined in Table 4. It is clear that the Langmuir isotherm (R^2 = 0.930–0.996) and D–R model (R^2 = 0.907–0.989) provided better linear fittings for the adsorption of nitrate than the Freundlich isotherm (R^2 = 0.747–0.972).

Table 4
Thermodynamics models for the removal of nitrate by different materials at initial pH 4.0 and 7.0

pH	Models	Parameters	SB-AE	PSB_{MIHM}-AE	PSB_{UP}-AE	PSB_{DH}-AE	PSB_{OP}-AE
4.0	Langmuir isotherm	q_m (mg/g)	57.5	95.7	68.9	75.2	75.3
		K_L (L/mg)	0.0346	0.0282	0.0311	0.0299	0.0326
		R^2	0.995	0.996	0.991	0.930	0.991
	Freundlich isotherm	K_F (mg/g) (l/mg)$^{1/n}$	9.45	11.2	11.3	12.7	12.2
		n	3.30	2.75	3.34	3.38	3.27
		R^2	0.747	0.923	0.831	0.827	0.820
	D-R model	$q_{m(D-R)} \times 10^3$ (g/g)	63.2	95.1	70.2	75.2	77.9
		$\beta \times 10^3$ (mol^2/kJ^2)	10.7	9.76	9.04	8.44	9.05
		E (kJ/mol)	6.83	7.16	7.44	7.70	7.43
		R^2	0.907	0.989	0.935	0.925	0.931
7.0	Langmuir isotherm	q_m (mg/g)	73.4	100.2	80.6	89.2	87.0
		K_L (L/mg)	0.0237	0.0306	0.0275	0.0266	0.0293
		R^2	0.988	0.994	0.987	0.979	0.982
	Freundlich isotherm	K_F (mg/g) (l/mg)$^{1/n}$	9.89	13.6	13.7	14.2	14.3
		n	3.05	2.96	3.47	3.34	3.37
		R^2	0.891	0.972	0.945	0.945	0.928
	D–R model	$q_{m(D-R)} \times 10^3$ (g/g)	71.9	91.7	73.3	80.4	80.9
		$\beta \times 10^3$ (mol^2/kJ^2)	9.88	7.68	7.01	7.19	7.29
		E (kJ/mol)	7.11	8.07	8.45	8.34	8.28
		R^2	0.981	0.979	0.975	0.979	0.981

In the Langmuir isotherm and D–R model, the coefficients reflecting the sorption capacity (q_e, and $q_{m(D-R)}$) at both pH 4.0 and 7.0 increased after applying pretreatments, and the pretreatment of MIHM demonstrated the largest nitrate adsorption capacity (Table 3).

In the Langmuir isotherm, the dimensionless equilibrium parameter was determined by using the following equation [38]:

$$r = \frac{1}{1 + K_L C_0} \tag{8}$$

Values of $r < 1$ obtained in this study represented favorable nitrate sorption by different materials. In the Freundlich isotherm, the values of $1/n$ in all satiations are smaller than 1, also reflecting the favorable nitrate sorption by different materials [39]. In the D–R model, the magnitude of E could be used as coefficient estimating the type of adsorption [38]. The values of E at a pH of 4.0 found in this study were less than or close to 8 kJ/mol, which indicated that nitrate sorption by different materials was dominated by physical adsorption as most surface sites were protonated at a lower pH. Yet, at the higher pH of 7.0, the values of E which were higher than 8 kJ/mol (except the data of nitrate removal by SB-AE) demonstrated that the nitrate sorption by PSB-AEs was dominated by ion exchange because more surface sites were available for nitrate removal.

4. Conclusions

Four pretreatments, including the MIHM, UP, DH, and OP, were applied to prepare AE based on SB using the ETM method. Studies of characteristics and nitrate removal ability of AE found positive influences of all pretreatments in the enhancement of nitrate removal ability and the microwave-induced hydrothermal pretreatment method resulted in the maximum improvement of nitrate removal efficiency. A pseudo-second-order model was found to adequately describe the kinetics of nitrate removal by AE. In addition, the Langmuir isotherm and D–R model were more suitable than the Freundlich isotherm in detailing nitrate removal by AE. The D–R model used in this study made clear that nitrate sorption by AE was dominated by physical adsorption at a lower pH of 4.0 and nitrate sorption by PSB-AEs was dominated by ion exchange at a higher pH of 7.0.

Acknowledgments

We gratefully acknowledge the financial support from the National Natural Science Foundation of China (21307075) and Postdoctoral Science Foundation of China (2013M531602).

References

[1] J.M. Hernández-Salas, M.S. Villa-Ramírez, J.S. Veloz-Rendón, K.N. Rivera-Hernández, R.A. González-César, M.A. Plascencia-Espinosa, S.R. Trejo-Estrada, Comparative hydrolysis and fermentation of sugarcane and agave bagasse, Bioresour. Technol. 100 (2009) 1238–1245.

[2] Y.R. Loh, D. Sujan, M.E. Rahman, C.A. Das, Sugarcane bagasse—The future composite material: A literature review, Resour. Conserv. Recycl. 75 (2013) 14–22.

[3] L. Sene, A. Converti, M.G.A. Felipe, M. Zilli, Sugarcane bagasse as alternative packing material for biofiltration of benzene polluted gaseous streams: A preliminary study, Bioresour. Technol. 83 (2002) 153–157.

[4] D. Szczerbowski, A.P. Pitarelo, A. Zandoná Filho, L.P. Ramos, Sugarcane biomass for biorefineries: Comparative composition of carbohydrate and non-carbohydrate components of bagasse and straw, Carbohydr. Polym. 114 (2014) 95–101.

[5] T.A.H. Nguyen, H.H. Ngo, W.S. Guo, J. Zhang, S. Liang, Q.Y. Yue, Q. Li, T.V. Nguyen, Applicability of agricultural waste and by-products for adsorptive removal of heavy metals from wastewater, Bioresour. Technol. 148 (2013) 574–585.

[6] A. Gupta, S.R. Vidyarthi, N. Sankararamakrishnan, Thiol functionalized sugarcane bagasse—A low cost adsorbent for mercury remediation from compact fluorescent bulbs and contaminated water streams, J. Environ. Chem. Eng. 2 (2014) 1378–1385.

[7] A. Gupta, S.R. Vidyarthi, N. Sankararamakrishnan, Concurrent removal of As(III) and As(V) using green low cost functionalized biosorbent—Saccharum officinarum bagasse, J. Environ. Chem. Eng. 3 (2015) 113–121.

[8] U.S. Orlando, A.U. Baes, W. Nishijima, M. Okada, Preparation of agricultural residue anion exchangers and its nitrate maximum adsorption capacity, Chemosphere 48 (2002) 1041–1046.

[9] U.S. Orlando, A.U. Baes, W. Nishijima, M. Okada, A new procedure to produce lignocellulosic anion exchangers from agricultural waste materials, Bioresour. Technol. 83 (2002) 195–198.

[10] M. Karimi, M.H. Entezari, M. Chamsaz, Sorption studies of nitrate ion by a modified beet residue in the presence and absence of ultrasound, Ultrason. Sonochem. 17 (2010) 711–717.

[11] W.-Y. Wang, Q.-Y. Yue, X. Xu, B.-Y. Gao, J. Zhang, Q. Li, J.-T. Xu, Optimized conditions in preparation of giant reed quaternary amino anion exchanger for phosphate removal, Chem. Eng. J. 157 (2010) 161–167.

[12] U.S. Orlando, A.U. Baes, W. Nishijima, M. Okada, Comparative effectivity of different types of neutral chelating agents for preparing chelated bagasse in solvent-free conditions, J. Clean. Prod. 12 (2004) 753–757.

[13] X. Xu, B.-Y. Gao, Q.-Y. Yue, Q.-Q. Zhong, X. Zhan, Preparation, characterization of wheat residue based anion exchangers and its utilization for the phosphate removal from aqueous solution, Carbohydr. Polym. 82 (2010) 1212–1218.

[14] A. Keränen, T. Leiviskä, B.-Y. Gao, O. Hormi, J. Tanskanen, Preparation of novel anion exchangers from pine sawdust and bark, spruce bark, birch bark and peat for the removal of nitrate, Chem. Eng. Sci. 98 (2013) 59–68.

[15] T. Leiviskä, A. Keränen, N. Vainionpää, J. Al Amir, O. Hormi, J. Tanskanen, Vanadium removal from aqueous solution and real industrial wastewater using cross-linked and quaternized pine sawdust, Water Sci. Technol. 72 (2015) 437–442.

[16] W. Song, B. Gao, T. Zhang, X. Xu, X. Huang, H. Yu, Q. Yue, High-capacity adsorption of dissolved hexavalent chromium using amine-functionalized magnetic corn stalk composites, Bioresour. Technol. 190 (2015) 550–557.

[17] Y.S. Koay, I.S. Ahamad, M. Nourouzi, T.G. Chuah, Ion-exchange adsorption of reactive dye solution onto quaternized palm kernel shell, J. Appl. Sci. 14 (2014) 1314–1318.

[18] A. Keränen, T. Leiviskä, O. Hormi, J. Tanskanen, Preparation of cationized pine sawdust for nitrate removal: Optimization of reaction conditions, J. Environ. Manage. 160 (2015) 105–112.

[19] X. Xu, B.-Y. Gao, Q.-Y. Yue, Q.-Q. Zhong, Preparation of agricultural by-product based anion exchanger and its utilization for nitrate and phosphate removal, Bioresour. Technol. 101 (2010) 8558–8564.

[20] N. Reddy, Y. Yang, Properties and potential applications of natural cellulose fibers from the bark of cotton stalks, Bioresour. Technol. 100 (2009) 3563–3569.

[21] W.-H. Chen, S.-C. Ye, H.-K. Sheen, Hydrolysis characteristics of sugarcane bagasse pretreated by dilute acid solution in a microwave irradiation environment, Appl. Energy 93 (2012) 237–244.

[22] M. Balat, H. Balat, C. Öz, Progress in bioethanol processing, Prog. Energy Combust. Sci. 34 (2008) 551–573.

[23] R. Chosdu, N. Hilmy, Erizal, T.B. Erlinda, B. Abbas, Radiation and chemical pretreatment of cellulosic waste, Radiat. Phys. Chem. 42 (1993) 695–698.

[24] M.M. Kabir, K. Rajendran, M.J. Taherzadeh, I. Sárvári Horváth, Experimental and economical evaluation of bioconversion of forest residues to biogas using organosolv pretreatment, Bioresour. Technol. 178 (2015) 201–208.

[25] S. Zhu, Y. Wu, Z. Yu, J. Liao, Y. Zhang, Pretreatment by microwave/alkali of rice straw and its enzymic hydrolysis, Process Biochem. 40 (2005) 3082–3086.

[26] C.-Y. Yang, T.J. Fang, Combination of ultrasonic irradiation with ionic liquid pretreatment for enzymatic hydrolysis of rice straw, Bioresour. Technol. 164 (2014) 198–202.

[27] Q.-Q. Zhong, Q.-Y. Yue, Q. Li, X. Xu, B.-Y. Gao, Preparation, characterization of modified wheat residue and its utilization for the anionic dye removal, Desalination 267 (2011) 193–200.

[28] Z. Aksu, G. Dönmez, A comparative study on the biosorption characteristics of some yeasts for Remazol Blue reactive dye, Chemosphere 50 (2003) 1075–1083.

[29] G. McKay, V.J.P. Poots, Kinetics and diffusion processes in colour removal from effluent using wood as an adsorbent, J. Chem. Technol. Biotechnol. 30 (1980) 279–292.

[30] A.S. Özcan, B. Erdem, A. Özcan, Adsorption of Acid Blue 193 from aqueous solutions onto BTMA-bentonite, Colloids Surf., A 266 (2005) 73–81.

[31] C. Namasivayam, R.T. Yamuna, Waste biogas residual slurry as an adsorbent for the removal of Pb(II) from aqueous solution and radiator manufacturing industry wastewater, Bioresour. Technol. 52 (1995) 125–131.

[32] G. Ramadoss, K. Muthukumar, Influence of dual salt on the pretreatment of sugarcane bagasse with hydrogen peroxide for bioethanol production, Chem. Eng. J. 260 (2015) 178–187.
[33] K. Nakanishi, Infrared Absorption Spectroscopy, Practical, Holden-Day, San Francisco, CA, 1962.
[34] D.H. Williams, I. Fleming, Spectroscopic Methods in Organic Chemistry, McGraw-Hill, London, 1995.
[35] A.-A.M.A. Nada, M. El-Sakhawy, S.M. Kamel, Infrared spectroscopic study of lignins, Polym. Degrad. Stab. 60 (1998) 247–251.
[36] W.J. Weber, J.C. Morris, Kinetics of adsorption on carbon from solution, J. Sanit. Eng. Div. ASCE 89 (1963) 31–59.
[37] M. Arami, N.Y. Limaee, N.M. Mahmoodi, Evaluation of the adsorption kinetics and equilibrium for the potential removal of acid dyes using a biosorbent, Chem. Eng. J. 139 (2008) 2–10.
[38] M. Mahramanlioglu, I. Kizilcikli, I.O. Bicer, Adsorption of fluoride from aqueous solution by acid treated spent bleaching earth, J. Fluorine Chem. 115 (2002) 41–47.
[39] W.T. Tsai, C.W. Lai, K.J. Hsien, Effect of particle size of activated clay on the adsorption of paraquat from aqueous solution, J. Colloid Interface Sci. 263 (2003) 29–34.